Biochemical Characterization and Nuclear Magnetic Resonance Structure of Novel α-Conotoxins Isolated from the Venom of *Conus consors*[†,‡]

Philippe Favreau,*[,§,||] Isabelle Krimm,[⊥] Frédéric Le Gall,[§] Marie-Joëlle Bobenrieth,[⊥] Hung Lamthanh,[@] Françoise Bouet,[@] Denis Servent,[@] Jordi Molgo,[$] André Ménez,[@] Yves Letourneux,[§] and Jean-Marc Lancelin*[,⊥]

Laboratoire de Synthèses et Etudes de Substances Naturelles à Activités Biologiques, Université de La Rochelle, Pôle Sciences, Av. Marillac, 17042 La Rochelle Cedex, France, Laboratoire de RMN Biomoléculaire associé au CNRS, Université Claude Bernard−Lyon 1 & Ecole Supérieure de Chimie Physique and Electronique de Lyon, Bâtiment 308G, F-69622 Villeurbanne, France, Département d'Ingénierie et d'Etudes des Protéines, CEA/Saclay, 91191 Gif sur Yvette Cedex, France, and Laboratoire de Neurobiologie Cellulaire et Moléculaire, UPR 9040, CNRS, 91198 Gif sur Yvette Cedex, France

Received November 30, 1998; Revised Manuscript Received March 2, 1999

ABSTRACT: Two novel α-conotoxins were purified and characterized from the venom of the fish-hunting cone snail *Conus consors*. These peptides were identified by screening HPLC fractions of the crude venom and by binding experiments with *Torpedo* nicotinic acetylcholine receptor. The toxins named α-CnIA and α-CnIB exhibited sequences of 14 and 12 amino acids, respectively. The α-CnIA represents the main α-conotoxin contained in the venom, whereas α-CnIB is present in a relatively small amount. Chemical synthesis of α-CnIA was carried out using the Fmoc methodology by selective disulfide bond formation. The biological activity of the toxin was assessed in fish and mice. The α-CnIA inhibited the fixation of iodinated α-bungarotoxin to *Torpedo* nicotinic acetylcholine receptors with an IC_{50} of 0.19 μM which can be compared to the IC_{50} of 0.31 μM found for the previously characterized α-MI isolated from the piscivorous *Conus magus*. The synthetic α-CnIA blocked spontaneous and evoked synaptic potentials in frog and mouse isolated neuromuscular preparations at sub-micromolar concentrations. Solution NMR of this toxin indicated a conformational heterogeneity with the existence of different conformers in solution, at slow and intermediate exchange rates relative to the NMR chemical shift time scale, similar to that reported for α-GI and α-MI. NMR structures were calculated for the major NMR signals representing more than 80% of the population at 5 °C.

Conus snail venoms represent a useful and rich source of small peptides, which alter the normal function of diverse receptors or ionic channels. The toxins isolated from a number of *Conus* species have been shown to inhibit different types of nicotinic acetylcholine receptors (nAChRs)[1] and sodium, potassium, and calcium voltage-dependent channels (*1*−*3*). Several families of conotoxins have been defined according to their cysteine framework and their pharmacological profile. The α-conotoxins are small peptides of 12−30 amino acids, usually folded by two disulfide bridges, which inhibit muscular or neuronal nAChRs. As a consequence of the high variability in the sequence of these toxins from one species to another, a number of α-conotoxins with original subtype specificity have been characterized. The α-conotoxin GI, isolated from *Conus geographus* (*4*), MI from *Conus magus* (*5*), SI from *Conus striatus* (*6*), and EI from *Conus ermineus* (*7*) all target the muscular nAChRs composed of the following five subunits: two α, β, γ, and δ. Several other α-conotoxins are high-affinity ligands of neuronal nAChRs, which have a combination of α subunits (α_2−α_6) and β subunits (β_2−β_4) or which are composed of identical subunits (α_7−α_9). The number of subunits identified so far allows the great diversity of nAChRs found in a variety of tissues. The α-conotoxin ImI, from *Conus imperialis* (*8*), selectively targets the α_7 subunit that forms a homomeric nicotinic receptor. Receptors composed of the $\alpha_3\beta_2$ subunits are potently blocked by the conotoxin MII, isolated from the venom of *C. magus* (*9*). Conotoxins PnIA and PnIB, both from *Conus pennaceus*, block *Aplysia* neuronal acetylcholine receptors (*10*). More recently, the α-conotoxin EpI, from *Conus episcopatus*, was characterized as a specific inhibitor of $\alpha_3\beta_2$ and $\alpha_3\beta_4$ nAChRs (*11*).

[†] This work was supported by the Direction des Recherches, Etudes et Techniques (Grant 95/024 to Y.L.), and by the Direction des Systèmes de Forces et de la Prospective (Grant 98/1051 to J.M.). P.F. and I.K. were supported, respectively, by fellowships from Centre National de la Recherche Scientifique-Direction des Recherches, Etudes et Techniques, and by the Ministère de l'Education Nationale, de la Recherche et de la Technologie of France.

[‡] The NMR coordinates of the structure have been deposited in the Brookhaven Protein Data Bank (file name 1b45).

* To whom correspondence should be addressed.

[§] Université de La Rochelle.

[||] Present address: Laboratoire de Neurobiologie Cellulaire et Moléculaire, UPR 9040, CNRS, 91198 Gif sur Yvette Cedex, France.

[⊥] Université Claude Bernard−Lyon 1 & Ecole Supérieure de Chimie Physique and Electronique de Lyon.

[@] CEA/Saclay.

[$] UPR 9040, CNRS.

[1] Abbreviations: nAChRs, nicotinic acetylcholine receptors; HPLC, high-performance liquid chromatography; α-Bgtx, α-bungarotoxin; ip, intraperitoneal; im, intramuscular; EPPs, endplate potentials; MEPPs, miniature endplate potentials; DQF-COSY, double-quantum filtered correlation spectroscopy; NOESY, nuclear Overhauser enhancement spectroscopy; rmsd, root-mean-square deviation; TOCSY, total correlation spectroscopy.

10.1021/bi982817z CCC: $18.00
Published on Web 04/24/1999

Unlike the α-neurotoxins from snake venoms, the α-conotoxins targeting the muscular nAChRs are relatively short peptides (12−30 amino acids instead of 60−75 in α-neurotoxins), which can easily be obtained by chemical synthesis. This family of conotoxins recently stimulated much interest because of their ability to selectively inhibit one of the two acetylcholine binding sites of the muscular nAChRs (*12*−*14*). Moreover, toxins of this family can be used as tools for discriminating phylogenetic differences between nAChRs of vertebrates (*6*) and have been shown to be very effective in probing the nAChR by photoaffinity labeling with considerable accuracy (*15*, *16*). The discovery of new high-specificity ligands will improve the understanding of the pharmacology, physiology, and structure−activity relationships of the nAChRs.

Our previous observation that the venom of the piscivorous *Conus consors* suppressed transmission from vertebrate neuromuscular junctions (*17*) prompted us to purify the toxin(s) present in the venom that could be responsible for the blockade of postsynaptic nAChRs. For this purpose, the crude venom was fractionated by reversed-phase HPLC and fractions were screened by binding experiments with *Torpedo* nAChRs and neuronal α_7 receptors. Two α-conotoxins were identified, and the major α-conotoxin present in the venom was synthesized and subjected to a physicochemical, pharmacological, and structural characterization. The biological activities on fish and mouse, the binding on nAChRs, and the effects on isolated frog and mouse neuromuscular preparations were investigated. The structure of the toxin, deduced from solution NMR, was compared to the structure of two α-conotoxins (α-GI and α-MI). Evidence for a conformational heterogeneity is reported, as indicated for α-GI and α-MI conotoxins (*18*, *19*).

EXPERIMENTAL PROCEDURES

Materials. Specimens of *C. consors* were collected in Chesterfield Islands (New Caledonia) and immediately frozen at −80 °C. The venom apparatus was dissected, and the venom was squeezed out from the venom duct with forceps. The crude venom was dissolved in H_2O/0.8% TFA and centrifuged for 15 min at 4000*g*. The supernatant was separated and lyophilized to give the extracted crude venom. All Fmoc-protected amino acids, 4-(2′,4′-dimethoxyphenylhydroxy)methylphenoxy polystyrene resin (Rink amide resin, 0.36 mequiv/g), were obtained from Novabiochem (Läufelfingen, Switzerland). 2-(1*H*-Benzotriazol-1-yl)-1,1,3,3-tetramethyluronium hexafluorophosphate was obtained from Novabiochem. *N*-Methylpyrrolidone, trifluoroacetic acid, and acetonitrile were from SDS (Peypin, France). Other solvents and chemicals were purchased from commercial sources and were of the highest purity commercially available. All HPLC purifications and analyses were performed at room temperature on a Thermo Separation Products high-pressure liquid chromatographer, equipped with a TSP UV-150 wavelength detector.

Amino Acid Analysis, Sequencing, and Mass Spectrometry. Peptide samples (0.8 nmol) were hydrolyzed by addition of 200 μL of 6 M HCl under vacuum and heating at 120 °C for 16 h. The hydrolysates were analyzed on an Applied Biosystems 130A automatic analyzer equipped with an on-line derivatizer (model 420A) for the conversion of the free amino acids into their phenylthiocarbamoyl derivatives. The purified peptides were sequenced using an Applied Biosystems 477A automatic microsequencer, and phenylthiohydantoin derivatives were identified using an Applied Biosystems 120A on-line analyzer. Before sequencing was carried out, S-pyridylethylation of α-CnIA was performed as previously described (*20*). A sample of 0.4 nmol of α-CnIA was used for sequence assignment. Electrospray ionization mass spectra (ESI-MS) were obtained on an API III+ mass spectrometer (Perkin-Elmer Sciex) equipped with a nebulizer-assisted electrospray source.

Chemical Synthesis. α-CnIA was synthesized by solid-phase methods on an Applied Biosystems-Perkin-Elmer (ABI-PE) 430A peptide synthesizer (Foster City, CA), using the Fmoc methodology. Chain elongation was performed step by step using 0.1 mmol of Rink amide MBHA resin (0.36 mequiv/g) and 1 mmol of Fmoc amino acid derivatives. Amino acids were activated by 2-(1*H*-benzotriazol-1-yl)-1,1,3,3-tetramethyluronium hexafluorophosphate according to FastMoc Chemistry methodology (ABI-PE). Side chain protecting groups were trityl for Cys3, Cys8, and His, acetamidomethyl for Cys4 and Cys14, butyloxycarbonyl for Lys, *tert*-butyl for Ser and Tyr, and Ng-2,2,5,7,8-pentamethylchroman-6-sulfonyl for Arg. After full assembly was completed, the linear peptide was cleaved from the resin by treatment with 10 mL of trifluoroacetic acid/*m*-cresol/thioanisole/triisopropylsilane (92.5/2.5/2.5/2.5) for 2 h. The linear peptide was purified by semipreparative HPLC. A two-step oxidation procedure was then carried out (*21*, *22*). The folded peptide was characterized by amino acid analysis and mass spectrometry.

In Vivo Bioassays. Toxicity was tested on the fish (*Gambusia affinis*) by intramuscular (im) injection of the toxin diluted in 5 μL of a saline solution (150 mM NaCl). The paralytic state of the fish was deduced from its inability to resist to a weak vortex current in a large beaker. Groups of Swiss Webster mice (25−30 g) were injected intraperitoneally (ip) with 100 μL of a saline solution (150 mM NaCl) containing different concentrations of the toxin. Quantification of the dose effect was performed as previously described (*21*, *23*). Data were plotted according to the linear equation $Y = A + BX$, where Y is the death time (in minutes) and X the inverse of the dose of toxin (in $nmol^{-1}$).

Binding to Acetylcholine Receptors. Binding assays were performed using [^{125}I]-α-bungarotoxin (210−250 Ci/mmol, Amersham) as a competitor. AChR-rich membranes were prepared from the electric organ of *Torpedo marmorata* according to the methods of Sobel et al. (*24*). α_7 receptors were obtained by expressing the chimeric cDNA (α_7-5HT$_3$), which was kindly provided by Pr. Changeux (Institut Pasteur, Paris, France), in HEK cells as described by Servent et al. (*25*). For *Torpedo* membrane preparation, the effect of the α-conotoxin CnIA on the initial rate of [^{125}I]-α-Bgtx binding was measured. The toxin was preincubated, at different concentrations, for 2 h with 3 nM active sites of receptors and filtrated 5 min after the addition of 2 nM [^{125}I]-α-Bgtx. For α_7 receptors, the toxin was incubated for at least 30 min with 250 μL of the cell suspension and filtrated 6 min after the addition of 15 μL of 100 nM [^{125}I]-α-Bgtx. The competition curves were fitted with the empirical Hill equation.

Electrophysiological Recordings. Left and right hemidiaphragms muscles with their associated phrenic nerves were isolated from Swiss Webster mice (20−25 g) that were killed by dislocation of the cervical vertebrae followed by immediate exsanguination. The two hemidiaphragms were separated, and each was mounted in a Rhodorsil (Rhône-Poulenc, St. Fons, France)-lined organ bath (2 mL volume) superfused with a physiological solution with the following composition: 154.0 mM NaCl, 5.0 mM KCl, 2 mM $CaCl_2$, 1.0 mM $MgCl_2$, 5.0 mM HEPES buffer, and 11.0 mM glucose. The solution gassed with pure O_2 had a pH of 7.4. The cutaneous pectoris muscle and associated nerve was removed from double-pithed male frogs (*Rana esculenta*) weighing 20−25 g and pinned to the base of a 2 mL tissue bath superfused with a standard solution containing 115.0 mM NaCl, 2.0 mM KCl, 1.8 mM $CaCl_2$, and 5.0 mM HEPES buffer (pH 7.25). In some experiments, excitation and contraction were uncoupled by treating the cutaneous pectoris neuromuscular preparations with 2 M formamide (*26*).

The motor nerve of the isolated neuromuscular preparations was stimulated via a suction microelectrode, adapted to the diameter of the nerve, with pulses with durations of 0.05−0.1 ms and supramaximal voltage (typically 3−8 V). These pulses were generated by a S-44 stimulator (Grass Instruments) linked to a stimulus isolation unit.

Membrane potentials and synaptic potentials were recorded from endplate regions at room temperature (22−24 °C) with intracellular microelectrodes filled with 3 M KCl (8−12 MΩ resistance) using conventional techniques and an Axoclamp-2A system (Axon Instruments, Foster City, CA). Recordings were made continuously from the same endplate before and throughout application of the conotoxin that was being tested. Electrical signals after amplification were displayed on a digital oscilloscope and simultaneously recorded on videotape with the aid of a modified digital audio processor (Sony PCM 701 ES) and a video casette recorder (Sony SLC9F). Data were collected and digitized with the aid of a computer equipped with an analogue and digital I/O interface board (DT2821, Data Translation) at a sampling rate of 25 kHz. Computerized data acquisition and analysis was performed with a program kindly provided by J. Dempster (University of Strathclyde, Strathclyde, Scotland). Endplate potentials (EPPs) and miniature endplate potentials (MEPPs) were analyzed individually for amplitude and time course. For each condition that was studied, three to six individual experiments were performed and the results were averaged to give the presented mean ± standard error of the mean (SEM). Statistical testing was performed by using the Student's *t* test with $p < 0.05$ being taken to indicate significance.

NMR Measurements. Five hundred fifty microliters of a 3−4 mM sample in 90% H_2O/10% D_2O was used for the NMR experiments at pH 4.1 (direct pH-meter reading at 25 °C). All the NMR spectra were recorded on a Bruker Avance DRX 500 spectrometer using a 5 mm (^1H, ^{13}C, and ^{15}N) triple-resonance probe head, equipped with a self-shielded *z*-gradient coil. Data were processed using Bruker XwinNMR or GIFA V.4 (*27*) software. Results from all two-dimensional experiments were recorded with 512 (t_1) × 1024 (t_2) complex data points. The spectral width was 10 ppm; ^1H chemical shifts were quoted relative to the solvent chemical shift at 5 °C (4.964 ppm). DQF-COSY (*28*), TOCSY (*29*, *30*), and NOESY (*31*, *32*) experiments were carried out at 5 °C. The mixing time was 80 ms for the clean-TOCSY experiment (*33*) and 150 and 300 ms for NOESY experiments. In TOCSY and NOESY experiments, the solvent signal was suppressed using the WATERGATE sequence using a 3-9-19 pulse sequence with *z*-gradients (*34*, *35*). In the case of the DQF-COSY experiment, a low-power presaturation was used during the relaxation delay. The quadrature detection in the t_1 dimension was achieved using the States−TPPI method (*36*).

NMR Restraints. Distance restraints were classified into four categories according to the cross-peak intensity of the NOESY spectrum at the 150 ms mixing time. Upper bounds were fixed at 2.7, 3.3, 5.0, and 6.0 Å for strong, medium, weak, and very weak correlations, respectively, and 0.3 Å was added in the case of NOEs involving HN protons (*37*). A NOE found in the 300 ms NOESY spectrum but not in the 150 ms NOESY spectrum was considered a very weak correlation. The possibility of spin diffusion was implicitly included in the level of error defined by categorizing the NOE upper bound limits. The intensities of the NOESY cross-peaks between H2,6 and H3,5 of tyrosines were used as references for the strong category. Pseudoatom corrections (*38*) for upper bounds were used for distance restraints involving methyl protons or spectroscopically degenerate methylene protons (+1 Å) and magnetically equivalent aromatic protons (+2 Å). The χ_1 dihedral angle restraints deduced from the stereospecific assignments of diastereotopic β protons (*39*, *40*) were 180 ± 60°, 60 ± 60°, and −60 ± 60°. The disulfide bonds were explicitly introduced as covalent bonds in the calculations.

Structure Calculations. Models of the peptide were calculated using X-PLOR version 3.851 (*41*) and were analyzed using MOLMOL 2.4 (*42*). A total of 80 structures were generated starting from random coordinates by a high-temperature simulated annealing protocol at 1000 K (*43*), using the *parallhdg.pro* force field of X-PLOR that does no take into account the attractive term of the van der Waals interactions or the electrostatic interactions. The structures that agreed with the force field and experimental restraints (no NOE violations of >0.2 Å) were further refined, using the full CHARMM22 force field of X-PLOR. An approximate solvent electrostatic screening effect was introduced by using a distance-dependent dielectric constant and by reducing the electric charges of the formally charged amino acid side chains (Arg, Lys, and His) and the N-terminus to 20% of their nominal charges defined in the CHARMM22 force field. After 1500 steps of conjugate gradient energy minimization, the dynamic was initiated at 750 K, equilibrated for 0.5 ps with 1 fs integration steps, and then coupled to a heat bath at 750 K, and the molecule was allowed to evolve for 10 ps before being cooled slowly to 300 K over a period of 5.4 ps and allowed to evolve again at this temperature for 15 ps. At the end, structures were energy minimized by being subjected to 1500 steps of the conjugate gradient algorithm. The force constant used for the NOE potential in both steps was 50 kcal mol^{-1} $Å^{-2}$.

RESULTS

Isolation and Biochemical Characterization of α-CnIA and α-CnIB. Crude venom of *C. consors* was fractionated by HPLC using a C18 reversed-phase column. The profile of

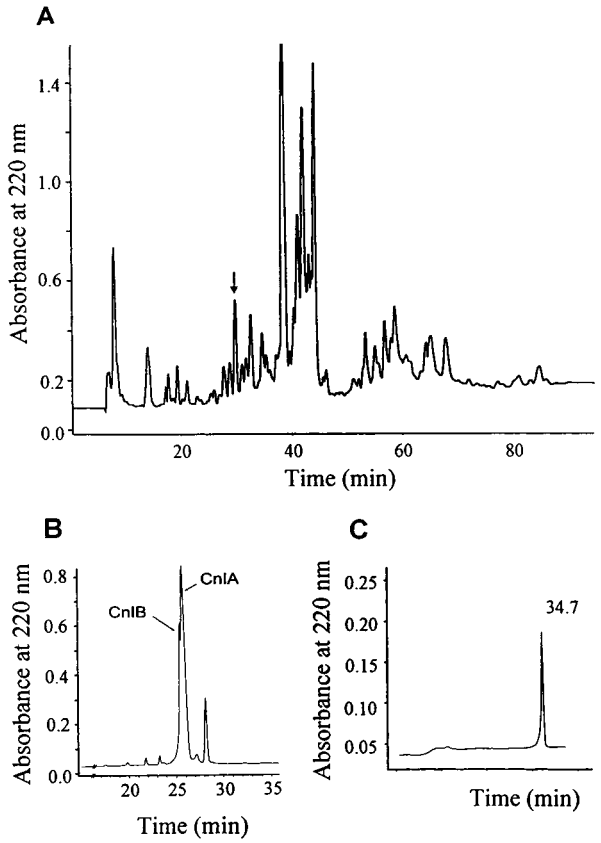

FIGURE 1: HPLC purification of α-conotoxin CnIA from *C. consors* venom. Buffer A was 0.1% TFA; buffer B was 0.1% TFA and 80% acetonitrile. (A) Crude venom was applied to a semipreparative C18 Vydac column. The gradient program was as follows: 0 to 8% B for 5 min, 8 to 80% B for 70 min, and 80 to 100% B for 10 min followed by 100% B for 10 min (flow rate of 2 mL/min). (B) Material eluting at 30.1 min (arrow, panel A) was re-run on an analytical C18 Vydac column with the following gradient program: 10 to 20% B for 10 min and 20 to 40% B for 40 min (flow rate of 1 mL/min). (C) Material corresponding to CnIA (panel B) was purified to homogeneity on an analytical C18 Vydac column (gradient program of 0 to 10% B for 10 min and 10 to 30% B for 60 min, with a flow rate of 1 mL/min).

the chromatogram (see Figure 1) showed a large number of components as it has been described in other *Conus* venoms, namely, *C. geographus* (*1*) or *C. striatus* (*44*). Our search for toxins that target the peripheral nicotinic receptor was guided by a screening of the main fractions from binding experiments with *Torpedo* nAChRs and α_7 nAChRs. On the peripheral nicotinic receptors, a positive and concentration-dependent response was obtained for a large peak eluting at 18% acetonitrile. Interestingly, none of the fractions tested on α_7 nAChRs exhibited a binding affinity of $<10\ \mu$M. The active fraction was further fractionated by analytical C18 HPLC, leading to two products displacing [^{125}I]-α-Bgtx on *Torpedo* nicotinic receptors with an estimated IC_{50} value in the micromolar range (not shown). Both toxins, present in an 80/20 ratio in the venom, were sequenced by Edman degradation to give two very similar peptides of 14 and 12 amino acids (Table 1). The minor peptide, α-CnIB, lacked the first two residues Gly and Arg when compared to the major toxin α-CnIA. To confirm the sequence and the position of the cysteines, native α-CnIA was reduced by dithiothreitol and pyridylethylated (see Experimental Procedures). The identity and the purity of both native toxins

Table 1: Main α-Conotoxins and Their nAChR Target[a]

Name	Sequence	nAChR target
CnIA	G R C C H P A C G K Y Y S C *	α/δ, α/γ
CnIB	C C H P A C G K Y Y S C *	
GI	E C C N P A C G R H Y S C *	α/δ, α/γ
MI	G R C C H P A C G K N Y S C *	α/δ, α/γ
SI	I C C N P A C G P K Y S C *	α/δ, α/γ
SII	G C C C N P A C G P N Y G C G T S	
MII	G C C S N P V C H L E H S N L C *	$\alpha_3\beta_2$
ImI	G C C S D P R C A W R C *	α_7
PnIA	G C C S L P P C A A N N P D Y C *	
EpI	G C C S D P R C N M N N P D Y"C *	$\alpha_3\beta_2$; $\alpha_3\beta_4$

[a] Asterisks denote an amidated C-terminus; quotes denote a sulfated residue.

were confirmed by amino acid analysis (results not shown) and electrospray ionization mass spectrometry, showing a mass of 1542.6 Da (theoretical of 1542.8 Da) for α-CnIA and 1328.8 Da (theoretical of 1329.5 Da) for α-CnIB. Mass results indicated an amidated C-terminus for both peptides as reported with almost all the known α-conotoxins (*7*). Conotoxins α-CnIA and α-CnIB are very similar with the previously described α-MI isolated from the piscivorous *C. magus* (*5*). α-CnIA has a Tyr in position 11, instead of an Asn as for α-MI. It can be assumed that α-CnIA and α-CnIB possess the same disulfide arrangement that is exhibited by this family of conotoxins, pairing Cys3 with Cys8 and Cys4 with Cys14 for α-CnIA. With the aim of fully characterizing the major toxin α-CnIA, peptide synthesis was carried out, as previously described (*22*). Successful synthesis of the desired synthetic α-CnIA toxin was confirmed by mass spectrometry (1542.7 Da for the synthetic product vs 1542.8 Da for the natural product) and coelution with the native peptide on analytical C18 HPLC. Moreover, in vivo tests confirmed the toxicity of the synthetic toxin.

In Vivo Bioassays. Bioassays were conducted on fish with im injections and on mice by ip injections of the synthetic α-CnIA. The LD_{50} was not estimated in fish, but 1 μg of α-CnIA (0.65 nmol) provoked paralysis in all fishes that were treated. In mice bioassays, α-CnIA induced flaccid paralysis followed by death. The rate of death was linearly dependent on the reciprocal dose of α-CnIA according to the equation $Y = A + BX$ (see Experimental Procedures). The following regression parameters were determined for α-CnIA: $A = 2.0$ and $B = 15.64$ ($r^2 = 0.98$). The specific activity deduced from the linear regression is 1.15 units/nmol. This can be compared to the specific activities of α-GI (1.5 units/nmol) and α-MI (4 units/nmol) (*21*).

Inhibition of [^{125}I]-α-Bgtx Binding to Nicotinic Receptors. The synthetic peptide α-CnIA was tested in vitro in a competition assay against [^{125}I]-α-Bgtx for the binding to peripheral and neuronal α_7 nicotinic receptors. All the experiments were performed by measurement of the initial rate of fixation of [^{125}I]-α-Bgtx on receptors preincubated with the synthetic toxins. Binding experiments with *Torpedo* nAChRs with α-CnIA gave an IC_{50} of 0.19 μM for the synthetic toxin (see Figure 2A). This toxin displays a slightly higher affinity toward the nAChR than α-MI (IC_{50} of 0.31 μM under the same experimental conditions). These values are in the range of those found for α-GI, α-MI, and α-SI

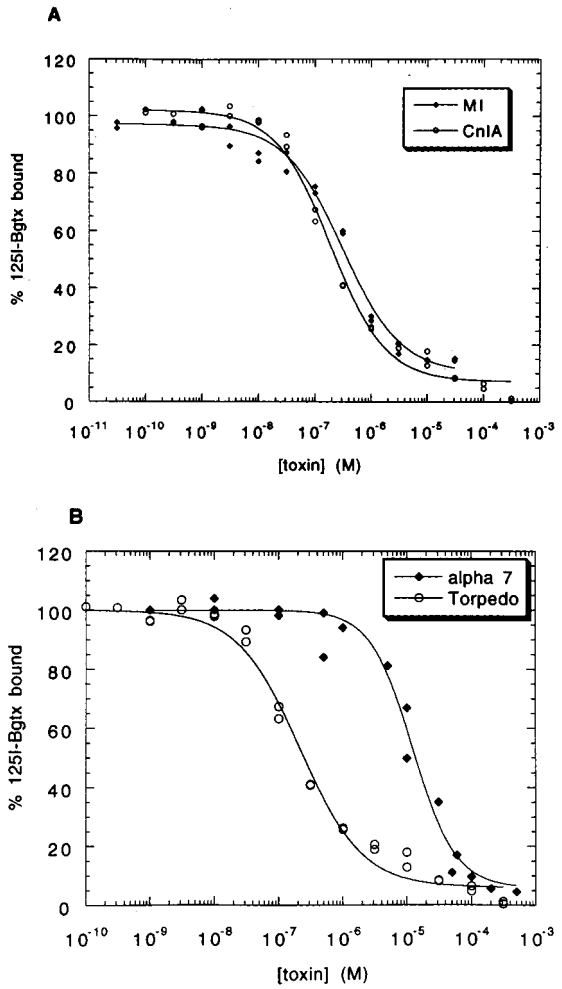

FIGURE 2: Competition binding assays with nAChRs. (A) Displacement of [^{125}I]Bgtx binding to *Torpedo* nAChR by synthetic α-conotoxins CnIA and MI. (B) Inhibition of [^{125}I]Bgtx binding to *Torpedo* nAChR and the neuronal α_7 nAChR. Each point represents the mean of results from two different experiments.

(*6*). Similar competition assays were performed on neuronal α_7 receptors. The difference in affinity between the muscular and the neuronal α_7 nicotinic receptors is 2 orders of magnitude (IC_{50} of 14.8 μM for neuronal α_7 and 0.19 μM for muscular nicotinic receptors of *Torpedo*) (see Figure 2B).

Blockade of Neuromuscular Transmission. The effects of synthetic α-CnIA on neuromuscular transmission were assessed on both isolated frog cutaneous pectoris nerve muscle preparation and mouse phrenic nerve hemidiaphragm muscle preparations, using electrophysiological techniques. Nerve stimulation of cutaneous pectoris muscles, previously treated with formamide to uncouple excitation−contraction coupling, elicited at junctional areas action potentials without contraction triggered by EPPs as shown in a typical recording (Figure 3A). Under these conditions, addition of 500 nM α-CnIA to the standard solution within a few minutes reduced the amplitude of EPPs, which could no longer reach the threshold for action potential generation in the muscle fibers, and finally completely blocked neuromuscular transmission (Figure 3A). A similar blockade of neuromuscular transmission by α-CnIA (500 nM) was observed in mouse phrenic nerve hemidiaphragm preparations in which excitation−contraction coupling was unaffected (data not shown).

The postsynaptic effect of α-CnIA on nAChRs was also

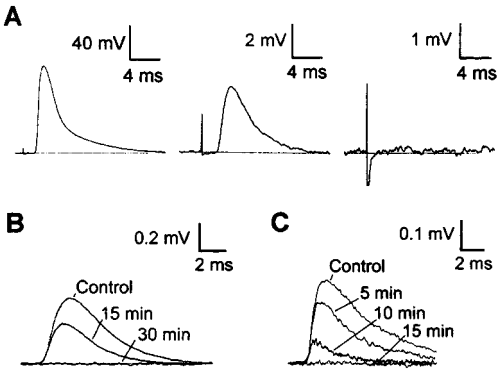

FIGURE 3: Blockade of neuromuscular transmission and of MEPPs by synthetic α-CnIA. Panel A shows an action potential elicited by single nerve stimulation (0.2 Hz) recorded just before the addition of 500 nM α-CnIA to the standard physiological medium (left trace), an EPP recorded 5 min after the addition of the toxin to the medium (middle trace), and the complete block of neuromuscular transmission after 60 min of toxin action (right trace). The resting membrane potential during the recordings on the frog cutaneous pectoris muscle was −78 ± 2.0 mV. Panel B shows in another frog cutaneous pectoris muscle the decrease in MEPP amplitude at different times after the addition of 300 nM α-CnIA to the medium. Each superimposed trace is the average MEPP amplitude. Data were obtained on the same junction. The resting membrane potential during recordings was −82 ± 1.5 mV. Panel C shows the time-dependent blockade of MEPPs by 300 nM α-CnIA in a mouse hemidiaphragm preparation. Each superimposed trace is the average of 10 MEPPs. The resting membrane potential during recording was −60 mV.

evident when recording spontaneous MEPPs in frog and mouse isolated nerve muscle preparations equilibrated in a standard physiological solution. Under these conditions, α-CnIA (100 nM) reduced the amplitude of MEPPs by about 33% in 30 min, without altering their frequency which indicates that the toxin, at this concentration, did not affect the spontaneous quantal transmitter release rate. Higher concentrations of α-CnIA (300 nM) completely blocked MEPPs, as shown in Figure 3 (panels B and C). The effects of α-CnIA reported here were reversible, provided preparations were washed for about 30 min with a toxin-free medium. Moreover, α-CnIA, in the range of concentrations that was studied (100−500 nM), had no consistent effect on the resting membrane potential of the muscle fibers in both frog and mouse isolated nerve muscle preparations (data not shown). The results obtained with α-CnIA when compared to those previously reported with α-GI (*45*) clearly indicate that α-CnIA on an equimolar basis is 6−8 times more potent than α-GI in blocking postsynaptic nAChRs at the frog neuromuscular junction.

NMR Resonance Assignment and Conformational Heterogeneity of α*-CnIA.* The sequence-specific resonance assignment (*38*) of the conotoxin α-CnIA was easily obtained. The chemical shifts observed at 5 °C are very similar to those previously reported for the α-conotoxin MI (*18*). The most important chemical shift differences for the Hα resonances were found for Lys10 and the mutated Tyr11 (0.09 and 0.12 ppm, respectively). The same but more pronounced phenomenon was obtained for the HN resonances. A chemical shift difference of 1.51 ppm was observed for Lys10. When the three-dimensional structure is examined (see below), it is clear that the HN proton is submitted to the ring current anisotropy of Tyr11, which causes a shielding of the resonance. Moreover, the mutation

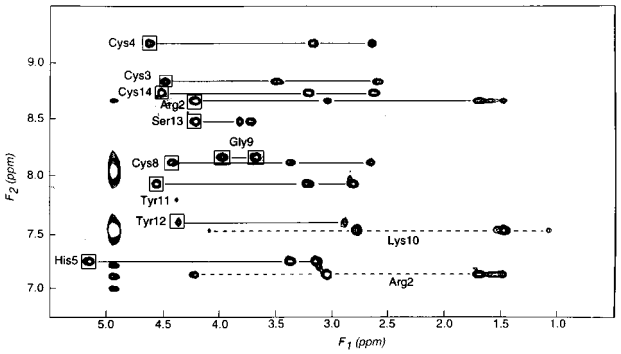

FIGURE 4: HN (F_2)−aliphatic (F_1) region of the 80 ms TOCSY spectrum of α-conotoxin CnIA recorded at 500 MHz in 90% H_2O/10% D_2O at pH 4.1 and 5 °C. Ten of the 12 observable spin systems are connected from the HN−Hα cross-peaks (in boxes). Ala7 and Lys10 residues indicate there is no HN to aliphatic magnetization transfer due to a very broad line width for the HN resonance. Dotted lines denote additional magnetization transfers involving NHδ and NHϵ of Arg2 and Lys10, respectively. Contours are plotted at a high level, showing the major spectrum. Minor signals can be detected at a lower level (see the text).

in α-CnIA suppresses the chemical shift degeneracy of Lys10 Hβ resonances observed in α-MI (*18*). Figure 4 shows the spin system assignment in the TOCSY spectrum of α-conotoxin CnIA recorded at 5 °C. The Ala7 HN resonance could not be observed, probably due to an extensive broadening of the corresponding line width. This resonance was also not observed in additional two-dimensional spectra recorded at 15 or 25 °C.

The one-dimensional spectrum, together with two-dimensional COSY and TOCSY spectra, indicated that the amide protons of the peptide have different line widths. The broadest lines were found for residues Cys4, Cys8, Lys10, and Tyr12. The Lys10 spin system could be observed in the HN−aliphatic region of the TOCSY spectrum. However, the transfer of coherence observed at 5 °C involved the ammonium NHϵ protons (Figure 4). The Lys10 amide proton resonance was very broad at 5 °C, and only a HN−Hα transfer was observed. At higher temperatures (15 and 25 °C), the amide proton resonance of Lys10 sharpened, and that of NHϵ broadened. This could be interpreted as a conformational exchange occurring around Lys10 HN at an intermediate rate on the chemical shift time scale, at 5 °C. This exchange becomes faster at room temperature, while the rate of chemical exchange of the ammonium protons with the solvent increases at the same time.

In addition to the major NMR signals detected in the two-dimensional spectra of α-CnIA (Figure 4), some minor NMR signals were found when two-dimensional contours were plotted at lower levels. Depending of the observed resonance, one or two other cross-peaks could be detected at 5, 15, and 25 °C (all resonances of Arg2 and Tyr12, HN−Hα resonances of His5, and terminal $CONH_2$ are the most obvious). No exchange connectivities could be observed between the major and minor forms in the NOESY spectra. This could indicate another conformational exchange phenomenon appearing very slow on the proton chemical shift time scale. This phenomenon was also observed in the structural study of α-conotoxin MI (*18*). For the major signals, NOE cross-peaks evidenced a trans peptide bond configuration for Pro6. Unfortunately, no NOEs could be assigned for the minor signals.

Table 2: Structural Statistics for the 43 NMR Structures of α-Conotoxin CnIA in H_2O at pH 4.1 and 5 °C

Cartesian coordinate rmsd (Å) vs the averaged coordinates of the (N, C^α, and C) backbone atoms of the 43 calculated structures	
residues 1−14	1.01 ± 0.24
residues 3−14	0.79 ± 0.16
mean number of distance restraint violation per structure	
>0.3 Å	0
>0.2 Å	0.02 ± 0.15
>0.1 Å	0.23 ± 0.43
X-PLOR potential energies	
F_{total} (kcal/mol)	123.2 ± 6.6
F_{bond} (kcal/mol)	5.9 ± 0.4
F_{angle} (kcal/mol)	29.4 ± 4.4
$F_{improper}$ (kcal/mol)	1.8 ± 0.5
F_{vdw} (kcal/mol)	−16.5 ± 4.1
F_{elec} (kcal/mol)	−217.0 ± 9.8
F_{DIHE} (kcal/mol)	72.6 ± 3.4
F_{NOE} (kcal/mol)	0.6 ± 0.5

Structure Calculations. Seventy-eight structurally relevant distance restraints, derived from the major NMR signals in NOESY experiments at 5 °C, were finally used for the structure calculations. They included 45 sequential (i, i+1), 19 medium-range (i, i+n, n < 5), and 14 long-range (i, i+n, n > 4) restraints. Dihedral angle restraints were also used to restrain two χ_1 angles for Cys3 and Tyr11 residues only. All other analysis of stereoscopically resolved diastereotopic methylene protons led to ambiguous stereospecific assignments. From 80 initial structures generated with the *parallhdg.pro* force field of X-PLOR, 50 were further refined with CHARMM22. A total of 43 structures were finally obtained. They agreed with both the experimental and force field restraints, as indicated in Table 2. They have no NOE violations exceeding 0.3 Å, and only one of the structures has one violation exceeding 0.2 Å. The models can be superimposed with a rmsd of 1.01 ± 0.24 Å for the backbone (N, C^α, and C) atoms for residues 1−14, and with a rmsd of 0.79 ± 0.16 Å for residues 3−14. Interestingly, the 43 calculated models share into two equally populated model families, differentiated by the backbone conformation in the Lys10−Tyr12 region of the peptide. The backbone torsion angles of Tyr11 (Ψ) and Tyr12 (Ψ and Φ) are dramatically different (Table 3). The χ_1 dihedral angle of Tyr12 is different in each conformer family. In the first family, it defines nearly systematically the trans rotamer ($\chi_1 = 180°$), whereas in the second family, the Tyr12 χ_1 angle is near 60°. The most specific differences between the two sets of models are summarized in Table 3.

Comparison with α-MI and α-GI Conotoxins. The conotoxin α-CnIA, which corresponds to an α-conotoxin MI Asn11 → Tyr mutant, is not structurally affected by the mutation. However, the secondary structure elements described in α-MI [the 3_{10} helix spanning residues 6−8 and the type I β turn involving residues 9−12 (*18*)] are not as well defined in the α-CnIA structure. The lack of NOE connectivities for HN of residues Ala7 and Lys10 due to the broad resonance line could be the origin of a less defined secondary structure (see the Discussion below).

The only structure of a homologous α-conotoxin available in the Protein Data Bank (*46*) is the X-ray structure of α-conotoxin GI solved at 1.2 Å resolution (*47*). The calculated models are similar to this X-ray model and can

Table 3: Structural Statistics for the Two Families of Structures in H_2O at pH 4.1 and 5 °C

	family 1 (22 structures)	family 2 (21 structures)
Cartesian coordinate rmsd (Å) vs the averaged coordinates of the (N, C^{α}, and C) backbone atoms		
residues 1−14	0.82 ± 0.24	0.92 ± 0.25
residues 3−14	0.59 ± 0.15	0.64 ± 0.12
Cartesian coordinate rmsd (Å) of the (N, C^{α}, and C) backbone atoms of the NMR models (residues 2−14) vs α-conotoxin GI (1−13) (*47*)	0.92 ± 0.28	1.40 ± 0.20
frequencies of occurrence of hydrogen bonds[a]		
Cys3 CO···NH Ser13	100%	100%
Gly9 CO···NH Tyr12	86%	not observed
Gly9 CO···NH Tyr11	77%	81%
Tyr12 CO···NH Cys14	59%	76%
Tyr11 CO···NH Ser13	75%	not observed
Ser13 Oγ···NH Cys3	68%	71%
His5 CO···NH Cys8	59%	67%
dihedral angles		
Tyr11 Ψ	8 ± 17	102 ± 40
Tyr12 Φ	−71 ± 11	−152 ± 30
Tyr12 Ψ	113 ± 13	169 ± 12
Tyr12 χ_1	−176 ± 8	−61 ± 31

[a] As detected with MOLMOL (*42*).

be superimposed with a rmsd of 1.16 ± 0.24 Å with respect to the backbone atoms of the X-ray GI structure. The first family (family 1 in the Table 3) is closest to the α-conotoxin GI structure compared to the second family, according to both rmsd superpositions and the dihedral angle values for Tyr11 and Tyr12 (Table 3) (*47*). The stereoview of the 22 models of this family is displayed in Figure 5, together with the superposition of the average coordinates of each family over the α-conotoxin GI X-ray structure in Figure 6.

DISCUSSION

Conus venoms represent a unique and abundant source of small and highly constrained peptide toxins targeting the nAChRs. Two new α-conotoxins were isolated from the venom of the piscivorous *C. consors* living in the Indo-Pacific region. Isolation of these toxins was allowed by a screening strategy based on binding competition on nicotinic receptors with [^{125}I]-α-Bgtx. Different screening methods have been devised to identify high-affinity binding ligands for nicotinic receptors, most of them relying on bioassays (*6*, *7*). This rapid and reliable screening with *Torpedo* nicotinic receptors and α_7 neuronal receptors expressed in HEK cells allowed direct assessment of the presence and specificity of two α-conotoxins from the *C. consors* venom. In producing large amounts of biologically active material, we were able to fully characterize the toxin by binding experiments, electrophysiology, and solution NMR.

Pharmacological and Structural Properties of Novel α-Conotoxins from C. consors. Conotoxins α-CnIA and α-CnIB possess a particular spacing of three and five amino acids between the cysteines, like GI, GIA, GII, MI, SI, SIA, and SII (*4*−*6*). All these α-conotoxins belong to the same $\alpha_{3/5}$ subclass in contrast with the $\alpha_{4/7}$ or $\alpha_{4/3}$ subclass, which include EI, EpI, MII, PnIA, PnIB, and ImI (*7*−*12*) (see Table 1). A striking similarity can be noticed between the two toxins isolated in the present study and conotoxin MI, only differing in the 11th position where a Tyr in α-CnIA and α-CnIB is replaced by an Asn in α-MI. Such a minor but original mutation does not lead to significant differences in the binding properties on *Torpedo* nAChRs. This is probably correlated with a very similar structure of α-conotoxins CnIA and MI according to their closely related chemical shifts (see the Results above). The NMR data recorded under similar conditions together with the structure calculations showed that the structure is not affected by the mutation.

Unfortunately, binding assays with *Torpedo* nicotinic receptors did not allow discrimination between the high- and low-affinity binding sites as has been previously reported with some other α-conotoxins (*13*, *48*, *49*). Amino acid mutation of a similar position in conotoxin SI led to a 10-fold decrease in the apparent affinity for one of the binding sites on *Torpedo* receptors (*12*). The Tyr residue in conotoxin

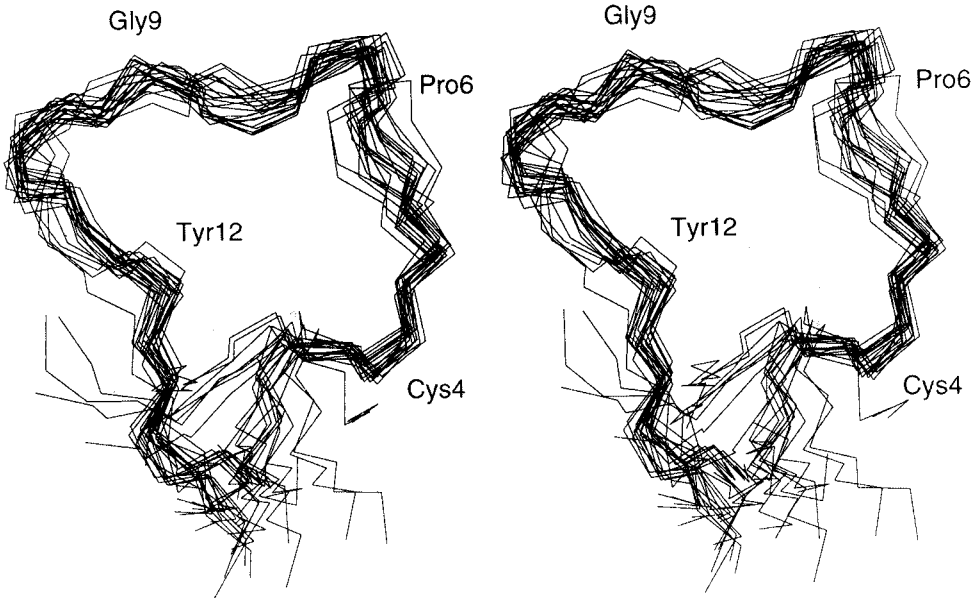

FIGURE 5: Stereoview of the 22 models of family 1 (see the text) of the 43 calculated structures of α-conotoxin CnIA according to the NMR data recorded at 5 °C. The 22 structures are superimposed for a minimum rmsd to the (C, Cα, and N) atoms from residues Cys3 to Cys14. The positions of residues Cys4, Pro6, Gly9, and Tyr12 are labeled.

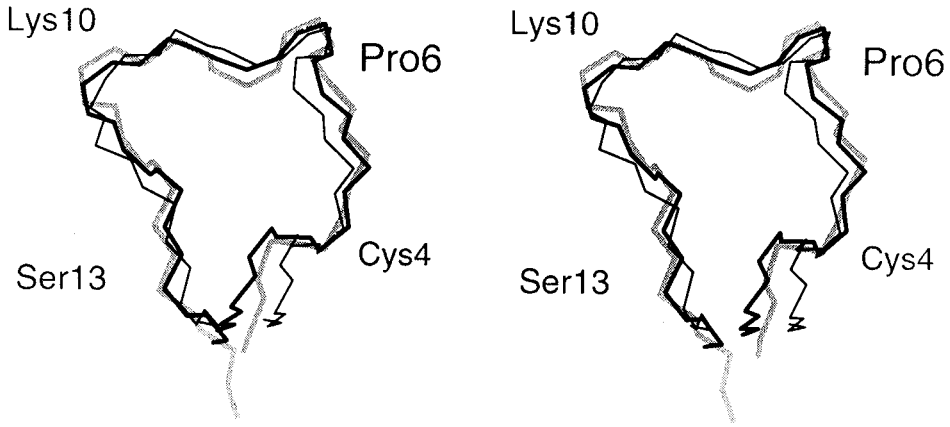

FIGURE 6: Backbone superposition for the averaged coordinates of family 1 (thick black line) and family 2 (thin black line) of the NMR structures of α-conotoxin CnIA (see the text) over the crystal structure of α-conotoxin GI (gray line; *47*) that contains one less amino acid.

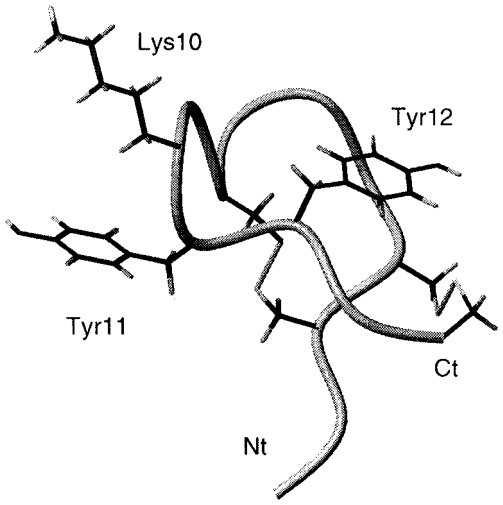

FIGURE 7: Representative model of family 1 of the 43 NMR structures of α-conotoxin CnIA. Side chains of Lys10, Tyr11, and Tyr12 are displayed, together with the two disulfide bridges. Nt and Ct denote the N-terminal and C-terminal ends, respectively.

α-CnIA may be relatively important to the affinity for the α or γ and α or δ sites compared to conotoxin MI. Further experiments could shed light on this interesting point. However, if differences in affinity would be obtained, they could be attributed to the nature of the amino acid side chain mutated in α-CnIA (N11Y), and not to a difference in the relative orientation of the side chain of residue 11 in both conotoxins. The Tyr11 side chain is solvent exposed (ca. 60% of the accessible surface), pointing into the solvent in tandem with the Lys10 side chain in the opposite direction of the Tyr12 side chain as shown in Figure 7. Tyr12 is less solvent exposed (ca. 30% of the accessible surface). The relative orientation of residues 10−12 is conserved in conotoxins α-GI and α-MI.

The 80-fold difference in the binding affinity between the muscular and neuronal α_7 receptor is in accordance with the lack of effects observed on ganglionic preparations with α-MI (*50*). The specificity for muscular versus neuronal nAChRs of α-CnIA has also been studied in bovine chromaffin cells where the synthetic α-CnIA (1 μM) was found to be unable to block the nicotine-evoked calcium influx in these cells (P. Favreau, C. Mattei, and J. Molgo, unpublished data). This can be compared to the inhibition of nicotine-induced catecholamines release in bovine chromaffin cells at sub-micromolar concentrations by α-EpI (*11*). Thus, α-CnIA appears to be a potent and selective blocker of the muscular subtype nAChRs as evidenced by electrophysiological recordings with amphibian and mammalian isolated neuromuscular preparations. Although little data is available concerning the effective doses of α-conotoxins on isolated neuromuscular preparations (*43*, *50*, *51*), our experiments with α-CnIA revealed some differences with respect to the effective concentrations needed to block nerve-evoked muscle contractions. Indeed, α-CnIA proved to be more potent than α-GI (*43*) in blocking the nerve-evoked synaptic potential and MEPPs occurring in frog cutaneous pectoris nerve muscle preparations. However, the effective dose that was found for inhibiting the synaptically mediated action potential by 50% (<500 nM for α-CnIA) is comparable to that reported by McIntosh et al. (*8*) for α-ImI (250−500 nM) which inhibits the neuronal α_7 nAChR. The results obtained with the phrenic nerve hemidiaphragm preparation provide the first recordings showing the blockade of MEPPs by an α-conotoxin. Previous studies with mammalian preparations have mostly relied on twitch tension recordings (*51*, *52*).

Conformational Heterogeneity in the α*-Conotoxins.* The structure calculation based on the NOE analysis of the major form sampled two families of conformers in the Lys10−Tyr12 segment as described in Table 3. The conformational heterogeneity could account for the specific broadening of Lys10 and Tyr12 HN resonances at a low temperature (5 °C), indicating an intermediate exchange rate on the NMR chemical shift time scale. Interestingly, in the NMR structural studies of α-conotoxin GI using a multiconformational approach (*19*), two distinct interconvertible conformers were found. The differences between the two conformations are only located in the Gly8−Cys13 region of the peptide (homologous to Gly9−Cys14 in α-CnIA), therefore including the sampled Lys10−Tyr12 region described in α-CnIA models.

An interesting feature during HPLC purification is the elution profile of native α-CnIA (Figure 1C) that is characterized by an asymmetric peak. Such asymmetry persisted even after re-running the late fraction of the peak. Interestingly, the same chromatographic behavior could be seen with the synthetic α-CnIA. Chromatography of the synthetic toxin at a low temperature (4 °C) demonstrated a minor peak eluting just before the major fraction (not shown). This chromatographic pattern is very similar to the one observed

for α-conotoxin MI and is interpreted as a slow interconversion occurring between two conformers (*19*).

This could correlate with the presence of some minor peaks detected in the two-dimensional NMR spectra. These minor species are in very slow exchange with the major form on the NMR chemical shift time scale. In many cases (His5 HN and terminal $CONH_2$), the frequency separations ($\Delta\delta$) between the different forms are about 20−50 Hz. This indicates an exchange rate constant $k \ll 2\pi\Delta\delta$ (i.e., $k \ll 100\ s^{-1}$) (*38*), which is compatible with the HPLC elution profile. Such a conformational exchange at a slow rate, in addition to the intermediate exchange described above, could originate from a very slow cis to trans isomerization of a peptidic bond. Unfortunately, no NMR data of such an isomerization were found here to support this hypothesis. Such heterogeneity was also found in the case of α-MI, as minor peaks in the NMR spectra of the conotoxin were also reported (*18*).

This study thus provides a new indication of the conformational diversity of α-conotoxins. In addition, our results point out the extensive variety of α-conotoxins present in the venoms of Conidae. The toxins characterized in this work provide information about the pharmacological potency of such toxins. Their extensive use as blockers of the muscular nAChRs is of considerable interest, and such well-defined probes may have a large number of applications.

ACKNOWLEDGMENT

We are grateful to Dr. C. Debitus, Dr. D. Laurent, the divers from ORSTOM (Noumea, New Caledonia), and the biologists from the Aquarium of La Rochelle for their help in collecting and acclimating the *Conus* species used in this work. We thank Xavier Trivelli for an excellent help in the structural analysis during a student summer stay in 1998 in Lyon.

REFERENCES

1. Olivera, B. M., Gray, W. R., Zeikus, R., McIntosh, J. M., Varga, J., Rivier, J., de Santos, V., and Cruz, L. J. (1985) *Science 230*, 1338−1343.
2. Olivera, B. M., Rivier, J., Clark, C., Ramilo, C. A., Corpuz, G. P., Abogadie, F. C., Mena, E. E., Woodward, S. R., Hillyard, D. R., and Cruz, L. J. (1990) *Science 249*, 257−263.
3. Gray, W. R., Olivera, B. M., and Cruz, L. J. (1988) *Annu. Rev. Biochem. 57*, 665−700.
4. Gray, W. R., Luque, A., Olivera, B. M., Barrett, J., and Cruz, L. J. (1981) *J. Biol. Chem. 256*, 4734−4740.
5. McIntosh, J. M., Cruz, L. J., Hunkapiller, M. W., Gray, W. R., and Olivera, B. M. (1982) *Arch. Biochem. Biophys. 218*, 329−334.
6. Zafaralla, G. C., Ramilo, C., Gray, W. R., Karlstrom, R., Olivera, B. M., and Cruz, L. J. (1988) *Biochemistry 27*, 7102−7105.
7. Martinez, J. S., Olivera, B. M., Gray, W. R., Craig, A. G., Groebe, D. R., Abramson, S. N., and McIntosh, J. M. (1995) *Biochemistry 34*, 14519−14526.
8. McIntosh, J. M., Yoshikami, D., Mahe, E., Nielsen, D. B., Rivier, J. E., Gray, W. R., and Olivera, B. M. (1994) *J. Biol. Chem. 269*, 16733−16739.
9. Cartier, G. E., Yoshikami, D., Gray, W. R., Luo, S., Olivera, B. M., and McIntosh, J. M. (1996) *J. Biol. Chem. 271*, 7522−7528.
10. Fainzilber, M., Hasson, A., Oren, R., Burlingame, A. L., Gordon, D., Spira, M. E., and Zlotkin, E. (1994) *Biochemistry 33*, 9523−9529.
11. Loughnan, M., Bond, T., Atkins, A., Cuevas, J., Adams, D. J., Broxton, N. M., Livett, B. G., Down, J. G., Jones, A., Alewood, P. F., and Lewis, R. J. (1998) *J. Biol. Chem. 273*, 15667−15674.
12. Groebe, D. R., Gray, W. R., and Abramson, S. N. (1997) *Biochemistry 36*, 6469−6474.
13. Sine, S. M., Kreienkamp, H. J., Bren, N., Maeda, R., and Taylor, P. (1995) *Neuron 15*, 205−211.
14. Kreienkamp, H. J., Sine, S. M., Maeda, R. K., and Taylor, P. J. (1994) *J. Biol. Chem. 269*, 8108−8114.
15. Myers, R. A., Zafaralla, G. C., Gray, W. R., Abbott, J., Cruz, L. J., and Olivera, B. M. (1991) *Biochemistry 30*, 9370−9377.
16. Myers, R. A., Cruz, L., Rivier, J., and Olivera, B. M. (1993) *Chem. Rev. 93*, 1923−1936.
17. Le Gall, F., Favreau, P., Richard, G., Letourneux, Y., and Molgo, J. (1999) *Toxicon 37*, 985−998.
18. Gouda, H., Yamazaki, K., Hasegawa, J., Kobayashi, Y., Nishiuchi, Y., Sakakirada, S., and Hirono, S. (1997) *Biochim. Biophys. Acta 1343*, 327−334.
19. Maslennikov, I. V., Sobol, A. G., Gladky, K. V., Lugovskoy, A. A., Ostrovsky, A. G., Tsetlin, V. I., Ivanov, V. T., and Arseniev, A. S. (1998) *Eur. J. Biochem. 254*, 238−247.
20. Tarr, G. E., Black, S. D., Fujita, V. S., and Coon, M. J. (1983) *Proc. Natl. Acad. Sci. U.S.A. 80*, 6552−6556.
21. Gray, W. R., Rivier, J. R., Galyean, R., Cruz, L. J., and Olivera, B. M. (1983) *J. Biol. Chem. 258*, 12247−12251.
22. Lamthanh, H., Virelizier, H., and Frayssinhes, D. (1995) *Pept. Res. 8*, 316−320.
23. Cruz, L. J., Gray, W. R., and Olivera, B. M. (1978) *Arch. Biochem. Biophys. 190*, 539−548.
24. Sobel, A., Weber, M., and Changeux, J. P. (1977) *Eur. J. Biochem. 80*, 215−224.
25. Servent, D., Winckler-Dietrich, V., Hu, H. Y., Kessler, P., Drevet, P., Bertrand, D., and Ménez, A. (1997) *J. Biol. Chem. 272*, 24279−24286.
26. del Castillo, J., and Escalona de Motta, G. (1978) *J. Cell Biol. 78*, 782−784.
27. Pons, J. L., Malliavin, T. E., and Delsuc, M.-A. (1996) *J. Biomol. NMR 8*, 445−452.
28. Rance, M., Sørensen, O. W., Bodenhausen, G., Wagner, G., Ernst, R. R., and Wüthrich, K. (1983) *Biochem. Biophys. Res. Commun. 117*, 479−485.
29. Braunschweiler, L., and Ernst, R. R. (1983) *J. Magn. Reson. 53*, 521−528.
30. Davies, D. G., and Bax, A. (1985) *J. Am. Chem. Soc. 107*, 2820−2821.
31. Jeener, J., Meier, B. H., Bachmann, P., and Ernst, R. R. (1979) *J. Chem. Phys. 71*, 4546−4553.
32. Macura, S., Hyang, Y., Suter, D., and Ernst, R. R. (1981) *J. Magn. Reson. 43*, 259−281.
33. Griesinger, C., Otting, G., Wüthrich, K., and Ernst, R. R. (1988) *J. Am. Chem. Soc. 110*, 7870−7872.
34. Piotto, M., Saudek, V., and Sklenar, V. (1992) *J. Biomol. NMR 2*, 661−666.
35. Sklenár, V., Piotto, M., Leppik, R., and Saudek, V. (1993) *J. Magn. Reson., Ser. A 102*, 241−245.
36. Marion, D., Ikura, M., Tschudin, R., and Bax, A. (1989) *J. Magn. Reson. 85*, 393−399.
37. Krimm, I., Gilles, N., Sautiere, P., Stankiewicz, M., Pelhate, M., Gordon, D., and Lancelin, J.-M. (1999) *J. Mol. Biol. 285*, 1749−1763.
38. Wüthrich, K. (1986) *NMR of proteins and nucleic acids*, Wiley-Interscience, New York.
39. Wagner, G., Braun, W., Havel, T. F., Schaumann, T., Go, N., and Wüthrich, K. (1987) *J. Mol. Biol. 196*, 611−639.
40. Hyberts, S. G., Marki, W., and Wagner, G. (1987) *Eur. J. Biochem. 164*, 625−635.
41. Brünger, A. T. (1996) *X-PLOR*, version 3.851, Yale University Press, New Haven, CT.
42. Koradi, R., Billeter, M., and Wüthrich, K. (1996) *J. Mol. Graphics 14*, 51−55.
43. Nilges, M., Clore, G. M., and Gronenborn, A. M. (1988) *FEBS Lett. 239*, 129−136.
44. Ramilo, C. A., Zafaralla, G. C., Nadasdi, L., Hammerland, L. G., Yoshikami, D., Gray, W. R., Ramachandran, J., Miljanich,

G., Olivera, B. M., and Cruz, L. J. (1992) *Biochemistry 31*, 9919−9926.
45. McManus, O. B., and Musick, J. R. (1985) *J. Neurosci. 5*, 110−116.
46. Bernstein, F. C., Koetzle, T. F., Williams, G. J. B., Meyer, E. F., Brice, M. D., Rodgers, J. R., Kennard, T., Shimanouchi, O., and Tamusi, M. (1977) *J. Mol. Biol. 112*, 535−542.
47. Guddat, L. W., Martin, J. A., Shan, L., Edmundson, A. B., and Gray, W. R. (1996) *Biochemistry 35*, 11329−11335.
48. Hann, R. M., Pagan, O. R., and Eterovic, V. A. (1994) *Biochemistry 33*, 14058−14063.
49. Groebe, D. R., Dumm, J. M., Levitan, E. S., and Abramson, S. N. (1995) *Mol. Pharmacol. 48*, 105−111.
50. Hashimoto, K., Uchida, S., Yoshida, H., Nishiuchi, Y., Sakakibara, S., and Yukari, K. (1985) *Eur. J. Pharmacol. 118*, 351−354.
51. Marshall, I. G., and Harvey, A. L. (1990) *Toxicon 28*, 231−234.
52. Blount, K., Johnson, A., Prior, C., and Marshall, I. G. (1992) *Toxicon 30*, 835−842.

BI982817Z